# Data processing of fibre-optic strain gauge data for axial pile load testing

Marijn Dekker [i)], Jeppe Christensen [i)], Iona Richards [ii)], Felix Schroeder [iii)] and Richard Jardine [iiii)]

i) Wood Thilsted Partners, Toldbodgade 51D, 3rd floor, 1253 Copenhagen K, Denmark.

ii) Wood Thilsted Partners, 1st Floor, 91-94 Lower Marsh, London, SE1 7AB, United Kingdom.

iii) Geotechnical Consulting Group LLP, 52A Cromwell Road, London, SW7 5BE, United Kingdom.

iiii) Imperial College, Department of Civil and Environmental Engineering, Skempton Building, London, SW7 2BB, United Kingdom.

## ABSTRACT

Field testing is invaluable for optimising pile design, particularly with new pile types, or unfamiliar or layered ground conditions. For axial pile load testing, axial shaft strain gauges can provide crucial extra information to enable more detailed test interpretation and answer key questions regarding piles' dynamic, cyclic or monotonic loading responses. Fibre-optic strain gauges offer advantages over conventional electrical resistance or vibrating wire gauges, including better survival rates, closer spacings and secure installation without needing to alter pile geometry. However, fibre-optic strain gauge data require significant processing to ensure good quality, physically meaningful information. This paper outlines strain gauge system selection and automated data processing applied to optimise test interpretation for a recent axial pile test campaign. The processing corrects for temperature variations, addresses scatter in spatial variations and identifies erroneous outlying data points. Successful processing relied on working from sound physical principles, observing and recording site operations meticulously and employing engineering judgement to help resolve anomalies that arose in the recorded datasets.

**Keywords:** Pile load testing, data processing, fibre-optic strain gauges, temperature effects

## 1 INTRODUCTION

Pile load testing and working pile monitoring are frequently undertaken to optimise and/or verify pile design. Deploying axial shaft strain gauges can provide crucial additional data to aid interpretation of monotonic and cyclic loading responses at a relatively modest additional cost. In axial tests, axial strain gauges can help identify the split between shaft and base resistance, while closely spaced strain gauges can determine distributions of shaft friction with depth. The latter is especially helpful in layered strata and with driven piles, where the local shaft friction varies strongly with relative height above the pile base (Jardine et al., 2005). In lateral tests, axial strain gauges can be used to resolve depth distributions of bending moments and lateral deflections; see Burd et al. (2020).

Axial strain gauge technologies include conventional electrical resistance (ER) and vibrating wire (VW) gauges as well as fibre-optic systems. Field experience has identified several challenges in obtaining high quality strain gauge data:

(i) the influence of temperature changes,
(ii) gauge and cabling survival rates under high water pressures and high accelerations imposed during driven pile installation, and
(iii) disturbance of the stress and strain fields around the pile caused by strain gauge systems, especially when bulky protective channels are introduced to improve gauge and cable integrity.

It is common for ER or VW gauges mounted on driven thin-walled open steel piles to suffer high gauge failure rates before testing commences, and great care is required to achieve tolerable outcomes; see Clarke (1993), Bica et al. (2014) or Vinck (2021). However, it proved possible to install many hundreds of fibre-optic gauges, configured in continuous embedded strings, on tens of open steel piles driven for the recent PISA and ALPACA Joint Industry Projects (JIPs) without any

significant incidence of premature failure; see Byrne et al. (2017), Jardine et al. (2019) or Burd et al. (2020).

This paper describes how fibre-optic strain gauge systems deployed for a recent industrial pile test campaign were selected and processed.

## 2 FIBRE-OPTIC GAUGE CONFIGURATION

The advantages of employing small-diameter fibre-optic strain gauge systems in continuous embedded strings extending down the full shaft lengths of driven thin-walled open steel piles are outlined by Doherty et al. (2015). Distinct strain measurements are obtained from short sections inscribed at the desired depths with Fibre Bragg Grating (FBG) techniques. Rather than relying on bulky instrument channels welded onto the piles to protect, for example, ER and VW strain gauges, the FBG gauges can be set in thin grooves machined along the pile length, giving a flush finish that does not alter the overall pile geometry. This allows the stress and strain fields developed around the instrumented test piles to be representative of working pile conditions. Provided care is given to how the FBG strings are attached and sealed in place, such installations can survive pile driving and provide exceptionally well-defined test data.

To cope with possible pile bending, at least two strings of fibre-optic gauges are required on opposing sides of each test pile. It is also helpful to add dedicated temperature gauges as thermal expansion of the pile and thermo-optic effects in the strain gauges affect the strain measurements. To be effective, temperature gauges should be insensitive to pile straining.

Expensive systems are required to read FBG gauges. Standard logging rate equipment is adequate for most monotonic and cyclic pile load testing programmes, including for the ALPACA JIP's cycle-by-cycle analysis of dual axis lateral cyclic tests. However, higher specification high-speed (5kHz) devices were required to capture the stress waves developed during the ALPACA pile driving and enrich the data gathered for signal matching analysis, see Buckley et al. (2020).

While FBG gauges were deployed on piles up to 1.8m diameter and 20m long for ALPACA, difficulties may arise in milling suitable grooves in significantly longer or larger diameter piles in some fabrication yards. Design engineers may be reluctant to allow grooves to be milled into the sides of working piles, unless persuaded that due allowance is made for their potential impact on the piles' structural performance and that stress concentrations generated by the grooves do not impact structural fatigue strengths significantly.

Furthermore, deployment on relatively rigid piles with large wall thickness to diameter ratios, as may be adopted for small-scale test piles, may not offer adequate strain measurement sensitivity. More sensitive surface-mounted ER, VW or FBG gauges may be required for such cases, noting that allowances should be made for these gauges' potentially significant failure rates.

The FBG techniques developed for the PISA and ALPACA JIPs were applied to a recent industrial pile test campaign. Ten test piles, with diameter and lengths approximately one-third of typical pin piles for offshore wind turbines' jacket substructures had FBG gauges installed into grooves cut in their 14 mm wall thickness. Two continuous fibres, with 20 roughly equally spaced strain gauges each, were installed in diametrically opposite grooves machined along each side of the test piles. In addition, 5 FBG temperature sensors were included on each side of the piles. The temperature sensors were placed on separate fibres from the strain gauges and installed separately in the pile groove.

## 3 PRINCIPLES OF DERIVATION OF AXIAL RESISTANCE FROM STRAIN

### 3.1 Poisson's straining effects

It is usual to interpret axial load distributions with depth by considering only the axial components of the structural pile loads. Axial load profiles with depth are found by multiplying measured axial strains by the pile's cross-sectional area and Young's Modulus. Variations in the axial load profile with depth then represent loads transferred from the pile to the surrounding soil by internal and external shaft resistance, as well as any end bearing component at the pile base.

This treatment, which may be adequate for many sites, implicitly ignores radial interactions with the surrounding soil mass. Poisson's ratio effects lead to radial expansion of the pile shaft out into the soil mass under compression and vice versa under tension. This may impact pile shaft resistance (see De Nicola and Randolph 1993) and lead to radial stresses building or falling on the pile shaft under loading, which lead to either axial extension of the shaft material under axial compression or the reverse under tension. Such Poisson's straining effects may impact the interpretation of loads from axial strain gauges in cases where very high radial stresses apply around pile shafts, for instance in dense sands; see Kolk et al. (2005). Adding circumferential strain gauges can assist in the interpretation of such second order effects.

For the recent pile test campaign, the ground conditions comprised less competent ground and it was not considered necessary to add circumferential strain gauges to account for Poisson's straining effects.

### 3.2 Internal shaft resistance

A key consideration in the interpretation of axial tests on open piles is the distribution of shaft friction between the internal and external shaft areas. While strain gauges placed on typical piles can only resolve the distributions of total (i.e. internally and externally transferred) shaft loads, special double-walled schemes can be employed to assess the components separately (Han et al., 2020). Other insights may be gained from dynamic analyses that employ separate inside, outside and plug resistance

models (Randolph (1993); Buckley et al. (2020)) and by comparing End of Driving shaft resistances with tension and compression tests conducted shortly after driving.

The internal shaft friction mobilised during tension tests that lift the internal core must be at least sufficient to carry the core weight, plus any reverse end-bearing developed across the core base. In the same way, the internal shaft friction developed during compression testing of fully plugged piles must, at least, match the vertical bearing capacity mobilised (at the interpreted overall pile failure point) across the core base.

For the recent pile test campaign, consideration of the above factors indicated that the piles' internal shaft resistances were significant, but considerably lower than those acting over the piles' outside shafts. Combining the core weight, pile weight and reverse end-bearing, the internal shaft resistance totalled 10–20% of total mobilised shaft resistance during monotonic tension loading. In determining the internal shaft resistance, the plug length ratio was estimated based on pile diameter and reverse end-bearing equal to the cavitation pressure at pile base; see Lehane et al. (2017).

## 4 PROCESSING OF RAW STRAIN DATA

The following sections consider how the strain gauge data from recent axial load tests were processed, taking account of the factors discussed above.

Initially, the data from strain gauges located diametrically opposite on each pile side were evaluated independently. This identified whether any pile had experienced significant bending during driving or testing and also allowed error checking of individual gauges.

Following these checks, the raw data was algorithmically processed. Different approaches were applied for (i) the step-wise monotonic and (ii) the continuously-varying sinusoidal cyclic loading tests.

### 4.1 Monotonic loading

The processing steps for monotonic tests were:

1. Temporal filtering of strain and temperature data
2. Removal of any steep temperature gradients
3. Temperature correction of strain data
4. Outlier detection and removal
5. Spatial filtering of strain data

*Step 1 – Temporal filtering of strain and temperature*

The strain and temperature gauge data are subject to small, rapid fluctuations on a timescale much shorter than that of the step-wise loading of the piles. These fluctuations are considered to be artefacts of the measurement system. The strain and temperature data were enhanced by applying a moving mean filter with a heuristically chosen window size of 20 seconds. This filter did not impact strain and temperature trends, but reduced the high frequency fluctuations.

*Step 2 – Removal of steep temperature gradients*

As outlined in Section 2, temperature gauges should be designed to be insensitive to the straining of the pile. However, the sensors deployed in the recent pile test campaign clearly reacted to pile loads, as seen in Figure 1, where Figure 1a shows raw temperature measurements and Figure 1b shows the corresponding loading pattern. The results imply an implausibly sharp increase in temperature with each load step, followed by partial apparent cooling between load steps. The close correlation between temperature and load makes it difficult to determine actual temperature variations, especially as the relationship between applied load and apparent temperature variation appears to be non-linear.

For stepwise load application, load-induced apparent temperature variations were removed by applying gradient-based processing to the temperature measurements. It was assumed that any local temperature-time gradients that exceed a heuristic cut-off limit of 5E-5°C/s represent the impact of pile loading on the instrument rather than true temperature data.

Figure 1c identifies the time periods where temperature gradients were assessed to be implausibly steep. Such periods were replaced by the mean of the remaining temperature gradients, computed using a multilinear fit, resulting in the corrected temperature signal shown in Figure 1d. Although the apparent cooling between each load application step were not removed by the above procedure, they may still reflect artefacts of the instrument behaviour – e.g. creep – rather than true physical changes.

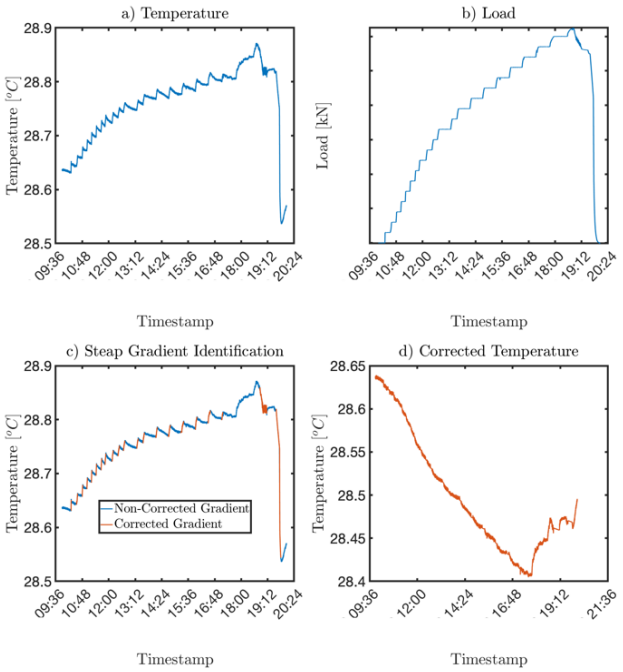


Fig. 1. Fibre-optic temperature gauge data: a) raw temperature-time signal, b) load signal, c) identification of implausibly steep temperature-time gradients, d) corrected signal.

The raw temperature data presented in Figure 1a suggest a maximum increase of around 0.25°C in the ground, but the corrected data in Figure 1d imply a similar magnitude decrease. The latter agrees with an independently measured decreasing ambient air temperature trend. Nonetheless, there is clearly scope for improving the design of fibre-optic temperature sensors to reduce their sensitivity to load-induced straining.

*Step 3 –Temperature correction of strain data*

Temperature corrections were made to all FBG strain data. Figure 2 demonstrates the impact of the temperature correction on strain for an example time series.

In general, the applied temperatures were interpolated linearly from the limited discrete (corrected) temperature measurements to the FBG strain gauge depth. However, this procedure was not appropriate for gauges located in areas where the external thermal boundary conditions changed sharply, e.g. at the ground water table level, or in pile sections exposed to direct sunlight and variable air temperature.

Once the temperature variation is identified, linear coefficients of thermal expansivity (α = strain/°C) are applied to correct for temperature. These coefficients may be based on theoretical or site-measured values. For the recent pile test campaign a value of α = 19$\mu\varepsilon$/°C was determined. This comprises both a contribution of the strain gauge response to temperature and the thermal expansivity of steel, which is typically in the range of 10–13$\mu\varepsilon$/°C. Some of the challenges in making such checks are discussed in Section 5.

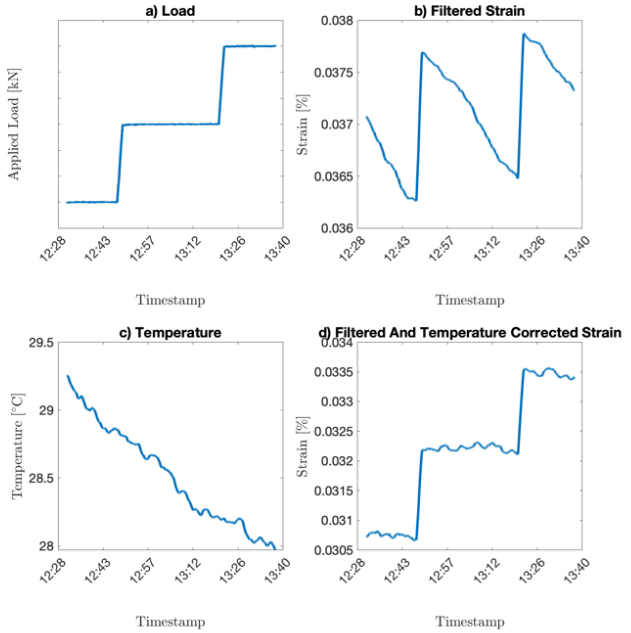


Fig. 2. Effect of temperature on strain measurement: a) applied load, b) time-filtered strain measurement, c) corrected temperature measurement, d) temperature-corrected strain measurement.

*Step 4 – Outlier detection and removal*

Several factors can cause errors in strain gauge records, leading to outlying data points that can mislead test interpretation. For the recent pile test campaign an iterative algorithm was applied to detect and remove such outliers. The algorithm applies a moving mean filter which runs through the strain data over the length of the pile for each individual timestep. A cut-off value is defined by an absolute norm, $p$, between the moving mean and the raw strain data; see Equation 1:

$$p = \sum_{i=1}^{N} \left\| \varepsilon_i - \varepsilon_{fit,i} \right\| / N \quad (1)$$

Where $N$ is the number of strain gauges along the pile, $\varepsilon_i$ are the strain data points and $\varepsilon_{fit,i}$ are the values of the moving mean fit.

If the absolute difference between any of the raw strain data points and the moving mean fit exceeds the computed value of $p$ multiplied by a heuristic scaling factor of 3, the point is classified as an outlier and removed for the next iteration. The algorithm is applied iteratively until no further strain data points are identified as outliers. For iterations where several strain data points are classified as outliers, only the outlier with the highest absolute difference to the moving mean fit is removed. The iterative process is illustrated in Figure 3.

It is noted that the detected outliers are inspected manually and, based on engineering judgement, some identified outliers might be kept in the data set.

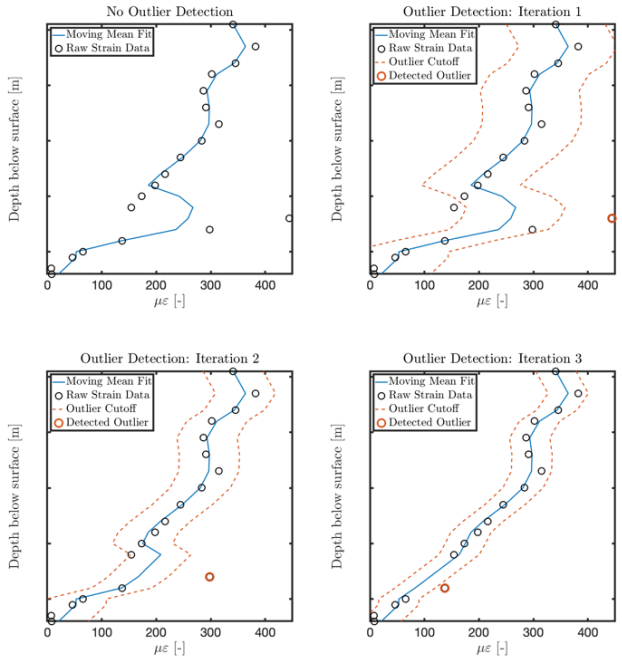


Fig. 3. Visualisation of the applied outlier detection algorithm with three initial iterations.

*Step 5 – Spatial filtering of strain data*

Spatial processing and filtering of the strain data was applied to obtain physically reasonable profiles with depth. First, the strain data relating to axial tension tests

was constrained to be zero at the pile base, neglecting any annular base reverse bearing capacity, and to match the strain corresponding to the applied load at any elevation above ground level. The weight of the pile and plug was considered to be fully resisted by internal shaft friction, see Section 3.2.

Second, the strain profile was constrained to keep total load increasing continuously from pile base to head, recognising that under monotonic loading, the shaft friction mobilised in the soil should oppose the applied loading over the full pile length. This assumption does not apply if negative skin friction develops due to consolidation (Alonso et al., 1984) or to piles undergoing unloading and subsequent reloading, as occurs, for example, during cyclic testing (see Section 4.2).

The spatial filtering to constrain the strain profile applied an iterative algorithm with a constrained least square fit, adopting piecewise linear regression between each strain gauge elevation. For the first iteration, nodes were included at each strain gauge elevation. In subsequent iterations, nodes which violated the requirement for continuous load increase from pile base to pile head were removed. Nodes closest to the pile head were removed first.

Although nodes were removed, the strain gauge data points were retained in the least square fitting for subsequent iterations. This process was repeated until strains increased monotonically from pile base to head.

### 4.2 Cyclic loading

For the continuously-varying sinusoidal cyclic loading tests performed in the recent pile test campaign, different processing approaches were taken for temperature effects (Step 3) and spatial filtering (Step 5), compared to that outlined for monotonic tests in Section 4.1. The axial cyclic tests in the recent pile test campaign included both one-way and two-way loading cases.

First, as described in Section 4.1 (Step 3), the fibre-optic temperature sensor measurements are undesirably impacted by loading. For the cyclic tests, there was no straightforward method to correct for this as pile head loads varied sinusoidally at a frequency of 0.1 Hz. Hence, it was considered more appropriate to apply no temperature correction than introduce arbitrary, potentially misleading adjustments.

Second, as described in Section 4.1 (Step 5), the spatial filtering applied for the monotonic loading tests constrained the strain and associated load measurements to increase monotonically upwards from the pile base. However, this physical constraint is not appropriate for cyclic loading because separate regions of the pile can experience tensile and compressive loading increments throughout the loading cycles. Instead, Savitzky-Golay filtering (Savitzky & Golay, 1964) with a heuristically selected window width of 8 was applied to the derived shear stress data to aid identification of the evolution of the pile-soil response.

## 5 FURTHER FACTORS TO CONSIDER WHEN APPLYING TEMPERATURE CORRECTIONS

In principle, thermal correction factors (α) may be established for test piles on site by lifting and suspending a pile vertically and recording how temperatures and strains vary over a suitable period of exposure to sunlight, under conditions of stable (self-weight) load.

Data recorded during such checks for the recent pile test campaign is shown in Figure 4. Temperatures were recorded on two sides of the pile (denoted A and B) at five elevations. Side A was exposed to direct sunlight and heated up by around 0.5°C over the two minutes measuring period, while the temperature on Side B remained constant (see Figure 4b). The corresponding variation in strain on side A is shown in Figure 4a for selected sensors; most sensors show increases in strain (extension) in line with the increasing temperature, but the two lowest sensors (19 & 20) show a reduction in strain (compression). Dividing the change in strain by the corresponding change in temperature (using linear interpolation and extrapolation), results in $\alpha$ values presented in Figure 4c.

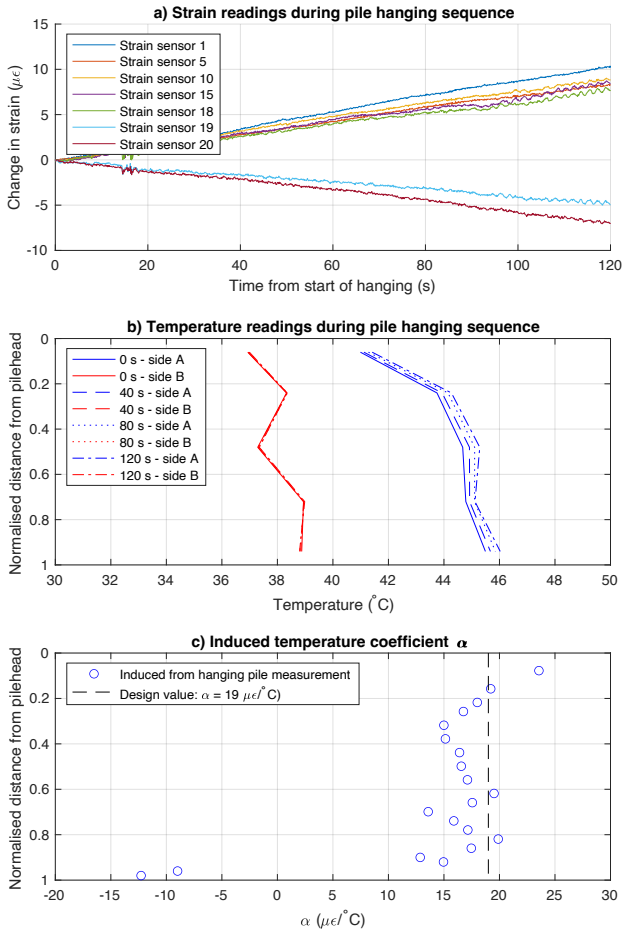


Fig. 4. Strain and temperature readings and indicative $\alpha$ values from a measurement of a pile hanging vertically from a crane.

While most of the measured $\alpha$ values lie within 20% of the design value of 19 $\mu\varepsilon$/ºC (see Section 4.1, Step 3), the two lowest sensors lead to anomalous negative $\alpha$ values. Closer analysis of site photographs shows that these gauges fell in the shadow of other site equipment during the checks. The misleading negative values of $\alpha$ resulted from an extrapolation of the linear trends from the exposed pile section into an area that was not heated in the same way due to shade from plant. This example illustrates the need to ensure any corrections applied to data have a sound physical basis and are correlated with careful recording of the site conditions and operations.

## 6 CONCLUSIONS

1. Field testing is invaluable for optimising pile designs, particularly with new pile types and unfamiliar or layered ground conditions.
2. Axial shaft strain gauges can add important extra information to enable more detailed test interpretation and help answer key questions regarding piles' dynamic, cyclic or monotonic loading responses.
3. Fibre-optic strain gauges offer advantages over conventional ER or VW gauges, including better survival rates, closer spacings and secure installation with less impact on pile geometry.
4. However, fibre-optic strain gauge data requires significant processing to ensure good quality, physically meaningful, information.
5. Automated processes are outlined to correct for temperature variations, address scatter in spatial variations and identify erroneous outlier data points.
6. The successful application of such procedures to optimise test interpretation relies on working from sound physical principles, observing and recording site operations meticulously, while also employing engineering judgement to help resolve anomalies that may arise in the datasets.

## REFERENCES


1) Alonso, E.E., Josa, A. and Ledesma, A. (1984): Negative skin friction on piles: a simplified analysis and prediction procedure, *Geotechnique,* 34(3), 341-357.

2) Bica, A.V.D., Prezzi, M., Seo, H., Salgado, R. and Kim, D. (2014): Instrumentation and Axial Load Testing of Displacement Piles. *Geotechnical Engineering* 167 (3), 238-252.

3) Buckley, R.M., McAdam, R.A., Byrne, B.W., Doherty, J.P., Jardine, R.J., Kontoe, S., and Randolph, M.F. (2020): Optimisation of impact pile driving using optical fibre Bragg grating measurements. *ASCE Journal of Geotechnical and Geoenvironmental Engineering*. DOI: 10.1061/(ASCE)GT.1943-5606.0002293

4) Burd, H.J., Beuckelaers, W.J.A.P., Byrne, B.W., Gavin, K.G., Houlsby, G.T., Igoe, D.J.P., Jardine, R.J., Martin, C.M., McAdam, R.A., Muir Wood, A., Potts, D.M., Skov Gretlund, J., Taborda, D.M.G. and Zdravković, L. (2020): New data analysis methods for instrumented medium scale monopile field tests. *Géotechnique*, 70 (11), pp 961-969.

5) Byrne, B.W., McAdam, R.A., Burd, H.J. Houlsby, G.T., Martin, C.M. Beuckelaers, W.J.A.P, Zdravkovic, L., Taborda, D.M.G, Potts, D.M., Jardine, R.J, Ushev, E., Liu, T.F., Abadias, D., Gavin, K., Igoe, D., Doherty, P., Skov Gretlund, J., Pacheco Andrade, M., Muir Wood, A., Schroeder, F.C, Turner, S. and Plummer, M. (2017): PISA: New Design Methods for Offshore Wind Turbine Monopiles. Keynote. *Proc 8th Int. Conf. on Offshore Site Investigations and Geotechnics, SUT London*. Vol. 1, p. 142-161.

5) Clarke, J. (1993): *Large-scale pile tests in clay*. Thomas Telford, London, p. 595.

6) De Nicola, A. and Randolph M.F. (1993): Tensile and compressive shaft capacity of piles in sand. *ASCE Journal of Geotechnical Engineering*. 119 (12), 1952-1973.

7) Doherty, P., Igoe, D., Murphy, G., Gavin, K. Preston, J., McAvoy, C., Byrne, B.W., Mcadams, R., Burd, H.J., Houlsby, G.T., Martins, M.C., Zdravkovic, L., Taborda, D.M.G., Potts, D.M., Jardine, R.J., Sideri, M., Schroeder, F. C., Muir Wood, A., Kallehave, D. and Skove Gretlund, J. (2015): Field validation of fibre Bragg grating sensors for measuring strain on driven steel piles. *Géotechnique Letters* 5, 74–79.

8) Han, F, Ganju, E., Prezzi, M., Salgado, R. and Zaheer, M. (2020): Axial resistance of open-ended pipe pile driven in gravelly sand. *Geotechnique*, 70 (2), 138-152.

9) Jardine, R.J., Chow, FC, Overy, RF and Standing, J.R (2005): *ICP design methods for driven piles in sands and clays*. Thomas Telford Ltd, London p. 105.

9) Jardine, R.J., Kontoe, S., Liu, T.F., Vinck, K., Byrne, B.W., McAdam, R.A, Schranz F. Andolfsson, T and Buckley, R.M. (2019): The ALPACA research project to improve design of piles driven in chalk. *Proc. XVII European Conf. Soil Mech. and Geotechnical Engg. Reykjavik, Iceland*. Pub. ECSMGE. DOI: 10.32075/17ECSMGE-2019-71.

10) Kolk, H.J., Baaijens, A.E., and Vergobi, P. (2005): Results of axial load tests on pipe piles in very dense sands: The EURIPIDES JIP. *Frontiers in Offshore Geotechnics*, Taylor & Francis, London, 661 – 667.

11) Lehane, H.J., Lim, J.K., Carotenuto, P., Nadim, F., Lacasse, S., Jardine, R.J. and Dijk, B.F.J. van. (2017): Characteristics of unified databases for driven piles. Keynote. *Proc 8th Int. Conf. on Offshore Site Investigations and Geotechnics, SUT London*. Vol. 1, p. 162-191.

12) Randolph M. F. (1993): Analyses of stress wave data from pile tests at Pentre and Tilbrook. *Large-scale pile tests in clay*. Thomas Telford, London, Ed. Clarke, J., 436-447.

13) Savitzky, A. and Golay, M.J. (1964): Smoothing and differentiation of data by simplified least squares procedures. *Analytical chemistry*, 36(8), 1627-1639.